Investigating chromatin structure using super-resolution microscopy

First Year EngD Report

Christophe Lynch

UCL

Table of Contents

List of acronyms and abbreviations used in this report

3C	Chromosome conformation capture
3D	Three-dimensional
5C	Chromosome conformation capture with carbon copy
(k/Mbp)	(Kilo- or mega-)base pairs
BrdU	Bromodeoxyuridine (5-bromo-2'-deoxyuridine)
DAPI	4',6-diamidino-2-phenylindole
DNA	Deoxyribonucleic acid
EdU	Ethynyldeoxyuridine (5-Ethynyl-2´-deoxyuridine)
EMCCD	Electron-multiplying charge-coupled device (image sensor)
G1-phase	Gap 1 phase (of the cell cycle)
HeLa	Henrietta Lacks (cell donor)
Hi-C	High-throughput chromosome conformation capture
M-phase	Metaphase (of the cell cycle)
(m)FISH	(multicolour) fluorescence in situ hybridisation
NA	Numerical aperture
OTF	Optical transfer function
PCR	Polymerase chain reaction
PSF	Point spread function
PVA	Poly vinyl alcohol
RESOLFT	Reversible saturable optical fluorescence transitions
sCMOS	Scientific complementary metal–oxide–semiconductor (image sensor)
SIM	Structured illumination microscopy
SMLM	Single molecule localisation microscopy
S-phase	Synthesis phase (of the cell cycle)
STED	Stimulated emission depletion

Investigating chromatin structure using super-resolution microscopy

1. Introduction

The human genome, of which the sequence is now fully known, comprises in total about two metres of DNA. What remains to be discovered, however, is precisely how such a length of DNA is organised within the cell nucleus, with a diameter of mere tens of microns, and how it is manipulated during the various phases of the cell cycle. Indeed, chromatin is a dynamic structure, folding and unfolding over generations as the cell carries out its functions and replicates. Accurate and timely replication of DNA is crucial to cell survival: a wide range of chromosome abnormalities are implicated in disease and genetic conditions, not least in cancers and the formation of tumours.

Whilst the basic units of organisation of chromatin are known at the molecular level, as well as larger macromolecular (micron scale) structures, in between we know little about how chromatin is arranged. In the region between one and one-hundred nanometres, there is much debate as to how chromatin, the complex formed between DNA and proteins, is folded. It is generally accepted that a 10 nm fibre – the 'beads on a string' structure of the nucleosome-DNA complex – exists, but whether or not this fibre condenses to form a thicker 30 nm fibre is controversial. The study of chromatin is therefore a very active field, with many different methods currently being applied.

The main focus of this project is on applying new microscopy methods to a particularly difficult structure. The most important initial questions are whether new optical techniques can be used to visualise the 30 nm fibre and the 10 nm fibre in chromatin, and, taking advantage of 3D capabilities, whether these structures have any bearing on the superstructure and function of chromosomes. So-called 'super-resolution' methods have been used to resolve features in cells on the order of 40 nm, which is far superior to conventional microscopy.

In this report, we will discuss new super-resolution microscopy methods and how they may be applied to the study of chromatin, and also touch on powerful new genetic methods of probing chromatin structure which could be used in conjunction with super-resolution imaging in the future. We will also present preliminary results obtained during the course of the project.

2. Review of methods used in the study of chromatin

Chromatin is ubiquitous in eukaryotes, with the basic nucleosome unit – a histone octamer around which is wrapped 150 base pairs of DNA – conserved across almost all eukaryotic species. As such, chromatin is a fundamental material and its study is of great interest. As with all structural biology, optical microscopy has played a great role in unravelling some of the mysteries associated with DNA, however in recent years the limits of light microscopes have become all too clear. Recent advances have allowed imaging of certain structures beyond the diffraction barrier, and the most popular and successful of these so-called 'super-resolution' methods will be described here. Other imaging techniques have met with success: electron[1,2] and helium ion microscopy,[3] atomic force microscopy[4] and assorted X-ray methods[5,6] have produced images of chromosomes with remarkable resolution, in some cases in three dimensions. Biomolecules contain significant amounts of metallic cations, and so secondary ion mass spectrometry imaging has been employed to visualise the distribution of such species within chromatin and chromosomes.[7] These techniques, whilst yielding impressive results, do not fall within the scope of this review, and so the reader is referred to publications cited and the references therein.

Although imaging is deeply important for understanding how biomaterials function, quantitative information can be obtained from spectroscopy and scattering experiments. Both X-ray[8] and neutron[9] scattering have been used to support arguments for and against the presence of certain levels of chromatin structure (the presence of the notorious 30 nm fibre, for example), however the lack of a consensus on these structures implies that these methods alone cannot be used to determine chromatin organisation. Indeed, the most significant advance in understanding chromatin structure in recent years perhaps came in the form of the 'C' methods pioneered by Job Dekker's laboratory.[10] These recently-developed genetic techniques have been used to build computational models of chromatin in different phases of the cell cycle, for the first time linking the genome to chromatin structure in a quantitative manner. The 'C' family of techniques – from chromosome conformation capture (3C) – shall be discussed in the following section.

2.1 The 'C' methods

Chromosome conformation capture (3C) was introduced by Job Dekker in the early years of this century as a technique to model the physical properties of the chromosome.[10] From these primitive elastic models, 3C and its related derivatives have evolved into sophisticated and complex procedures to generate models of chromatin interaction at different scales. All follow

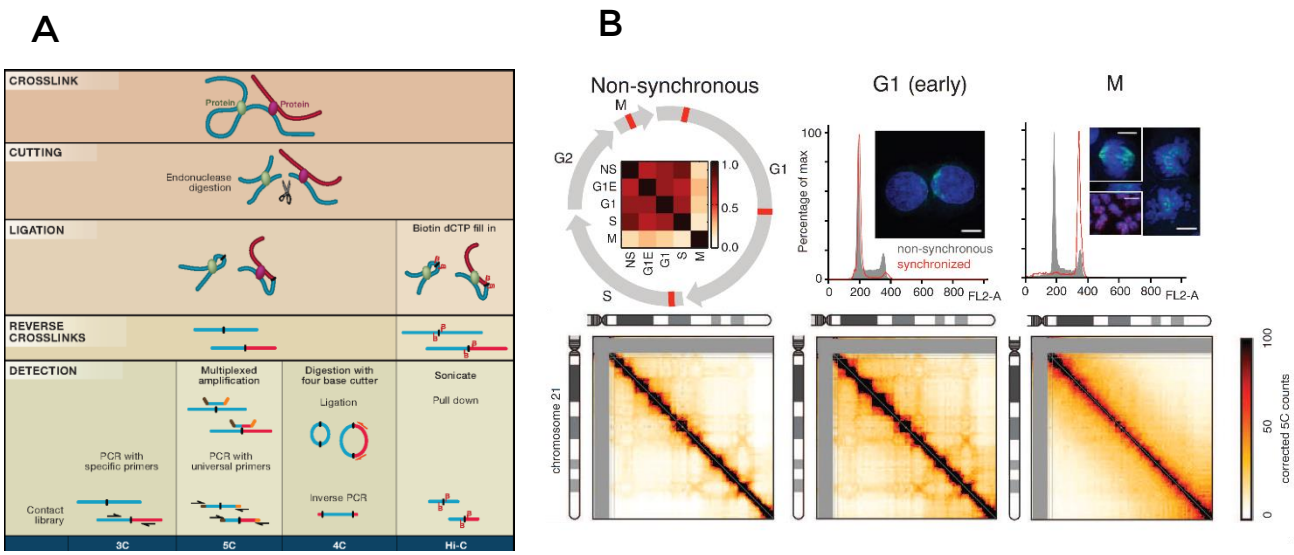

Figure 1

A) C-methods share the same basic principles: proximal DNA is cross-linked then a restriction enzyme cuts through the strands. Ligation is used to join free ends of the linked DNA strands; in the case of Hi-C, the ligation step is used to introduce a reactive biotin group for detection and subsequent purification. Crosslinks are reversed, resulting in a 'new' DNA fragment comprising the two sections of DNA which originally touched. The sequence of these fragments is determined using PCR or high-throughput sequencing.

B) Hi-C heat maps showing contacts between different regions on the genome in human chromosome 21. In the G1 phase of the cell cycle, there are contacts between specific loci on the genome, reflecting the relatively open chromatin structure. As the cell reaches metaphase, chromosomes condense, shown by an increased number of contacts in the Hi-C heat map.
Adapted from Hakim and Misteli[11] *and Naumova*[16].

the same basic procedure (figure 1.A): DNA is cross-linked by treatment with formaldehyde or a similar agent, before being dissected by a restriction enzyme, leaving linked fragments of DNA with two free ends each. These linked fragments will not necessarily be close in the genome; rather, only DNA which is *spatially* close will be linked. Free ends from the joined fragments are ligated, then the crosslink is reversed, yielding a new fragment made up of the two linked sequences. By one of various means, the sequences of the linked DNA fragments are identified (sequencing, polymerase chain reaction [PCR] assay etc.).[11]

In reality, the differences between the techniques lie in which interactions are probed: the original 3C method requires the loci being probed to be known, a necessity when using sequence-dependent PCR primers, limiting it to 'one versus one' interactions. 5C (chromosome conformation capture with carbon copy) improves on this by using universal PCR primers, allowing interactions between non-specific loci to be investigated.[12] Hi-C provides a truly genome-wide dataset by virtue of a novel purification step. Instead of using primers to capture ligated sequences, a magnetic bead is incorporated into the DNA fragments during the ligation step.[13] Fragments marked with this bead can be extracted and sequenced with ease, allowing all occurring interactions to be studied, rather than just those specified by a PCR primer.

In the case of 5C and Hi-C experiments, chromatin interaction data can be displayed in the form of a heat map (figure 1.B): a matrix is formed showing the probability of contact occurring

between different regions of the genome.[13–15] Such maps can be made for both intra- and inter-chromosomal contacts. The dominant feature of the heat maps is the strong diagonal resulting from the interaction between fragments in close proximity on the genome, however striking patterns do emerge away from the diagonal. Furthermore, studying heat maps of the same chromosome/section of the genome at different phases of the cell cycle shows clear changes in chromatin organisation. In a recent high-profile publication, it was shown that simulated Hi-C datasets of polymer model chromosomes obtained using molecular dynamics could be correlated with experimental data, providing evidence for a loop-based folding model of chromatin.[16] It should be noted that Hi-C data risk being influenced by sample averaging artefacts or other systematic errors: the technique requires the averaging of conformational data from millions of cells. Recently, Peter Fraser's group performed Hi-C on single cells,[17] showing that significant variations occur between different cells of the same type. This is not to say that conventional Hi-C data is not valid, but care must be taken when interpreting data to ensure that conclusions made reflect the nature of the experiment. Hi-C and the related techniques are impressive and have certainly reignited interest in chromatin structure. Whilst there is still debate as to whether or not single-cell methods are superior to studies on averaged populations, it is perhaps true that verification of genetic data will only be achieved by comparing results to high-resolution images.

2.2 Super-resolution optical microscopy

Since the latter part of the 19th century it had been assumed that resolution in microscopy was limited by the diffraction of light. The limit was defined by Abbe as a function of the numerical aperture of the imaging system and the wavelength of illuminating light:[18]

$$d = \frac{\lambda}{2n \sin\theta} = \frac{\lambda}{2\,\mathrm{NA}}$$

where d is the size of the smallest resolvable feature, λ is the wavelength of incident light, n is the refractive index of the medium and sin θ is the angle of the maximum cone of light that can enter the lens, with the numerical aperture, NA, of the system defined as $n \sin\theta$.[19,20] Practically, this means a resolution of no better than around 200 nm can be achieved with a standard fluorescence microscope (assuming a wavelength of ~400 nm and NA of 1.4 at best). In recent years, methods have been developed to circumvent the Abbe limit, with startling results: under optimum conditions, resolutions of 6 nm have been achieved using modified confocal microscopes.[21] Other modified fluorescence microscopes can routinely resolve features separated by distances of less than 50 nm. Whilst all such 'super-resolution' methods are based on existing fluorescence microscopes, they can be divided into two categories: 'functional' super-resolution takes advantage of fluorophore photophysics to engineer the point spread function (PSF, the

term given to the function which describes the profile of light captured by a system; for a microscope the PSF is typically Gaussian in shape) of the optical system, or interferes with fluorescence characteristics to allow individual molecules to be localised; 'true' super-resolution encompasses methods where improvements in resolution originate in the optics of the system, rather than being dependent on the fluorescence of the dyes or lack thereof. We discuss notable applications of super-resolution imaging to the study of chromatin in the following section, preceded by a brief overview of popular super-resolution methods.

2.2.1 Stimulated emission depletion microscopy (STED)

STED[22,23] is an implementation of Stefan Hell's RESOLFT (reversible saturable optical fluorescence transitions) principle,[20,24] where reversible switching between two states of a fluorophore allows for emitted light to be attributed to fluorophores at a specific coordinate of the sample. STED limits the effective emission profile of fluorophores to a spot smaller than the diffraction limit using two lasers aligned about the same point; the excitation laser acts as normal, exciting dyes to the excited singlet state, while a depletion laser with a toroidal profile acts to stimulate emission from the excited singlet state, forcing dyes within its range to remain in the ground state.[25] The toroidal depletion beam leaves only a central spot 50 nm in diameter from where fluorescence is emitted (figure 2). This spot is scanned in a rastering mode across the sample to build up an image.

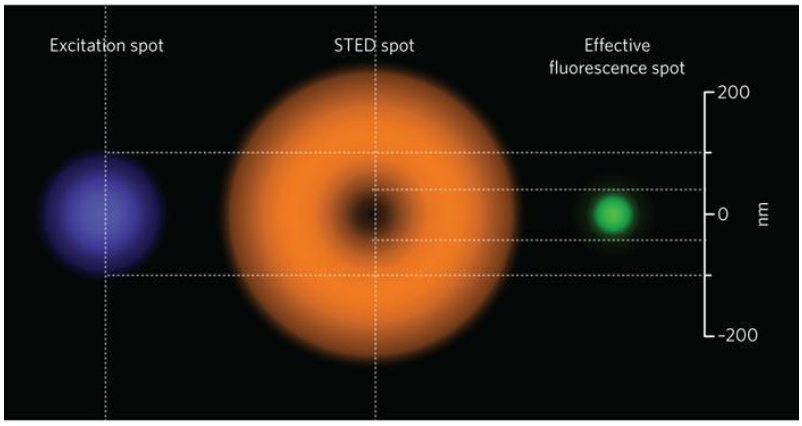

Figure 2
The principle behind STED microscopy: A toroidal depletion laser (orange) is aligned with the excitation beam (blue). All fluorophores within the range of the depletion 'doughnut' cease to fluoresce, resulting in a smaller effective excitation spot (green). Reproduced from Abbott.[25]

Whilst STED allows for an impressive increase in resolution, notable drawbacks include the slow nature of acquisition, inherited from confocal microscopy, and the necessity of irradiating often sensitive samples with high intensity lasers. Parallelisation methods are currently being developed to decrease acquisition time, which will address both the length of time needed to obtain an image and in turn the amount of time the sample is exposed to the lasers.[26–28] It should also be noted that specialised bright, photostable dyes are required for successful imaging.

2.2.2 Single molecule localisation microscopy (SMLM)

Single molecule localisation microscopy fulfils the RESOLFT principle in a different way to STED. Rather than forcing molecules to stay in a non-emissive state with a depletion laser, fluorophores cycle between a fluorescent state and a dark state at random.[29–31]At any given time, the majority of molecules will be in the non-emissive dark state, whilst a small subset will stochastically recover to fluoresce. The small subset of fluorophores will be spatially separated, allowing individual molecules to be resolved against the dark background of the image. Light which passes through the optical system will be observed by a detector, usually an EMCCD or sCMOS camera as a Gaussian point spread function (PSF), which can be modelled during post processing, the centroid of the PSF determined and the position of the fluorophore in the image plane recorded as a set of coordinates. In the vast majority of cases, the PSF can be approximated by a Gaussian distribution, and this is reflected in the plethora of localisation software available for SMLM data analysis: many algorithms apply Gaussian masks[32,33] when searching for fluorophores in a frame. Alternatively, some software will employ curve-fitting algorithms such as Levenberg-Marquardt[34,35] iteration or a centre-of-mass[36] algorithm to fit a profile to the recorded fluorophores. It is the precision with which individual emitters can be localised that affords SMLM its tenfold increase in resolution over standard microscopy: the fact that a point can be localised with a precision of 10 nm allows objects on that scale to be resolved.[37]

As different fluorophore subsets switch between the 'on' and 'off' states, the number of localised fluorophores increases until a point is reached when a reconstruction of the whole sample can be made (figure 3). In practice, with frames acquired at around 33 Hz, an experiment will take about five minutes to complete, with about 10,000 frames being captured. Obviously the number of frames needed to reconstruct an image depends on the number of fluorophores imaged in each; the greater the number of fluorophores localised per frame, the fewer frames needed for reconstructing an image. There is a trade-off between speed of acquisition and ease of reconstruction: necessarily, dense data will be prone to localisation errors, as overlapping

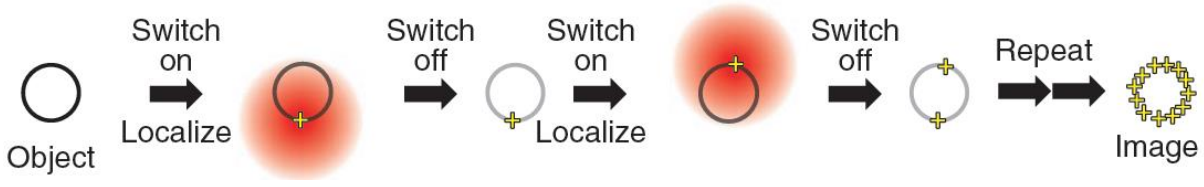

Figure 3
SMLM: An object is labelled homogeneously with fluorophores. These begin in a dark state, and fluoresce individually and stochastically (switch on) before returning to a dark state (switch off). Fluorophores are localised as they turn on. The process repeats enabling an image to be reconstructed from the fluorophore coordinates. Reproduced from Dempsey et al.[31]

fluorophores can be mistaken for single ones. Images are reconstructed simply by plotting the recorded fluorophore coordinates and blurring them with a Gaussian function.[38] The profile of the Gaussian used can be fixed, yielding a homogeneous image, which may be useful in cases where broad measurement of structures is required. However, when imaging complex structures, it is more typical to weight the Gaussian profile at each point according to the localisation precision and the number of photons collected, yielding a better idea of the topology of the sample. Typically, the greater the number of photons collected, the larger the amplitude of the Gaussian plotted and the brighter the spot on the reconstructed image.

Whilst in theory the task of localising spots against a dark background should be simple, in practice the analysis is complicated by various factors.[39,40] Dyes can be localised more than once in error, if for example they appear in multiple frames. With the effect of drift, such localisation errors can be compounded and the localisation precision subsequently reduced. Conversely, dyes can be permanently bleached before they are imaged, meaning they are never localised and thus never contribute to the final image. The density with which a sample is labelled can also be a problem, as it can be difficult to discriminate between different fluorophores.[41] In such cases, background signal can be strong, and depending on the type of camera used, noise can be significant. Many of these problems can be circumvented by ensuring that sample preparation is adequate and that imaging conditions are optimal. In the case of noisy or densely-labelled datasets, great strides have been made in developing algorithms for localising true fluorescence events amongst the erroneous signals. Notable are the 3B[42,43] algorithm which employs Bayesian statistics and a hidden Markov model to probe the likelihood of fluorophores switching between on and off states at given times, and DAOSTORM[44,45] which fits candidate molecules with multiple model PSFs of different shapes, allowing for identification of overlapping PSFs.

As SMLM becomes more widespread, sample preparation improves and conditions for achieving reliable on-off switching of dyes become optimised. Further improvements will come with the development of new algorithms for analysis, and crucially the sample preparation required to obtain useful images. To date, SMLM has been largely limited to what could be considered 'ideal' samples: the technique works well for discrete and well-defined structures such as well-separated fibres[46] within the cell and small, regular structures like clathrin-coated pits.[47] Such structures are 'ideal' for imaging as improvements in resolution allow for discrete, repeated structures to be viewed individually. More complex and continuous structures, like chromatin, remain difficult to image using SMLM. Chromatin lacks a repeating structure that can be labelled consistently and without damaging the material. In the next section we will discuss replication labelling, which allows regions as small as 10 kilo base pairs (kbp) in size. Imaging

small sections such as these could yield valuable information about the relation of chromatin structure to DNA replication.

2.2.3 Structured illumination microscopy (SIM)

SIM can be considered a 'true' super-resolution technique – rather than applying PSF engineering or attempting to discriminate individual molecules against a dark background, fluorescence information which would otherwise be lost to diffraction in a standard microscope is recovered by illuminating the sample with coherent, collimated light in a sinusoidal pattern, hence the name of the technique.[48] Interference of the light emitted from the sample with the structured illumination pattern encodes the 'lost' frequencies in the captured information. Varying the phase of the illumination by moving it across the sample allows for enough information to be acquired for a series of linear equations to be solved and the higher frequency information recovered.

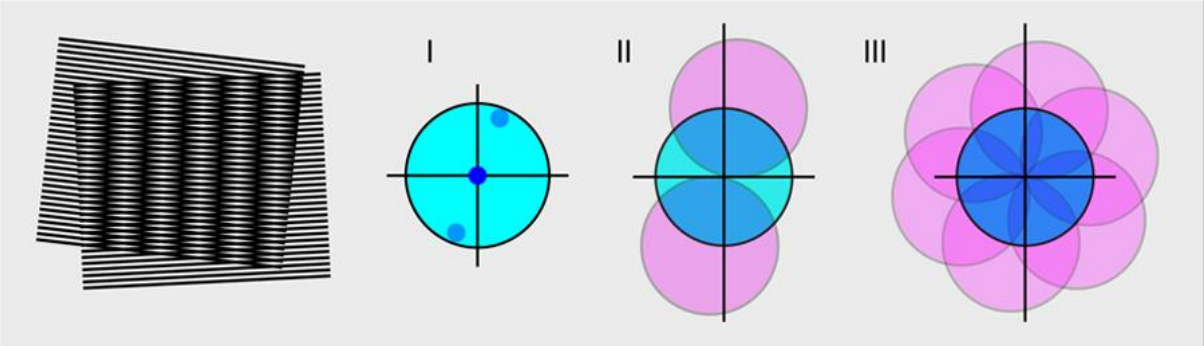

Figure 4
A diffraction grating is used to project a striped illumination pattern across the sample; this pattern interferes with fluorescence emitted by fluorophores on the sample. Ordinarily, the Fourier space sampled by the microscope (I, light blue circle) is limited by the optical transfer function of the system. Interference between the first order diffraction spots (I, small blue circles) and sample fluorescence leads to sampling of regions of Fourier space outside the OTF-defined boundary (II, pink circles). Sampling is only increased in one direction, so rotation is required to obtain an increase in resolution in all directions (III). Reproduced from Blom and Widengren.[48]

In a typical SIM system, the patterned light is achieved by placing a diffraction grating in the beam path.[49–51] Diffracted light from the grating is focussed onto the back focal plane of an imaging objective, blocking all but the zero and two first-order diffraction beams in the process. These three beams form three mutually coherent wavefronts upon leaving the objective, and their interference is viewed on the sample as a sinusoidal pattern. Variations in phase and orientation of the pattern are made by displacing the grating in space and by rotation.

Whilst acquisition of data is relatively straightforward, analysis is less so. Consider a typical microscope: fluorophores on a sample are excited and emit light. This light follows a path to an objective lens where it is focussed onto an imaging plane for recording. The image recorded

can be represented as a signal, *E(r)*, the fluorescence emission as a function of spatial coordinate r.

$$E(r) = [D(r) \cdot I(r)] \otimes \mathrm{PSF}(r)$$

E(r) is the product of the local fluorophore concentration *D(r)* and the illumination intensity *I(r)* convolved with the point spread function, PSF (r) of the optical system.[52] Analysis takes advantage of the convolution theorem: a convolution of two functions in real space is equivalent to their multiplication in the frequency domain, and similarly a multiplication of functions becomes a convolution. Having made a Fourier transform of the image, we can equally represent it mathematically as:

$$\tilde{E}(k) = [\tilde{D}(\vec{k}) \otimes \tilde{I}(\vec{k})] \cdot \mathrm{OTF}(\vec{k})$$

where terms with a tilde indicate the Fourier transform of their real-space counterparts as a function of k-vectors, and OTF (optical transfer function) is the Fourier transform of the microscope PSF. In a standard microscope, the illumination expression takes a trivial value and $\tilde{E}(\vec{k})$ depends locally on the term $\tilde{D}(\vec{k})$ at and only at a given point $\vec{k}$. In practice this means that only information from frequencies within a certain region of Fourier space is included in the image. The resolution of an image is therefore defined by the radius of the region in the Fourier transform of the image. The maximum observable spatial frequency, k_0 is given by:

$$k_0 = \frac{2\,\mathrm{NA}}{\lambda}$$

Where λ is the wavelength of the emitted light. If, however, the illumination expression has a non-trivial value, $\tilde{I}(\vec{k})$ exhibits a non-local dependence on points at values of $\vec{k}$ plus a distance, *d*, which is outside the observable region. In effect, information otherwise lost to diffraction is 'shifted' to lower frequencies.[50,51] Taking a sinusoidal illumination pattern:

$$I(r) = I_0[1 + \cos(k_0 \cdot r + \Phi)$$

(with I_0 the excitation illumination and Φ the phase of the illumination pattern) and convolving its Fourier transform with that of the fluorophore distribution, we obtain

$$\tilde{E}(\vec{k}) = I_0\left[\tilde{D}(\vec{k}) + 0.5\tilde{D}(\vec{k} + \overrightarrow{k_o})e^{i\phi} + 0.5\tilde{D}(\vec{k} - \overrightarrow{k_o})e^{-i\phi}\right]$$

such that each point k in frequency space has three Fourier components corresponding to the central spot and the two first-order diffraction spots (figure 4.I), which appear at the edge of the region in frequency space available to the microscope, $\vec{k} \mp \overrightarrow{k_o}$. [52] In order to obtain a high-

resolution image, the higher frequencies must be shifted back to their original positions. At each point k we have three unknowns, and so shifting the phase of the grating three times yields three linear equations which can be solved to obtain values for $\widetilde{D}(\vec{k})$ and $\widetilde{D}(\vec{k} \mp \overrightarrow{k_0})$. Having obtained these values, a real space image can be reconstructed.

The extra information we have gained from the structured illumination is only in one dimension, however. In order to extend the area sampled Fourier space, the diffraction grating is rotated and the imaging process repeated, usually three or five times (figure 4.III). The end result is a doubling of the size of frequency space sampled and therefore a doubling of resolution.[50,51] A SIM experiment involves the acquisition of at minimum nine images (three rotations and three phase shifts), however it is often desirable to perform five phase shifts with five rotations. Thus, photobleaching can be a problem – if the fluorescence intensity of the sample varies during acquisition, residual patterns from the structured illumination can be left on the reconstructed image.[53] This is a common problem in SIM, mediated by using stable fluorophores, however in general care should be taken when performing experiments to minimise the likelihood of artefacts. In general, it is wise to perform quality control during the course an experiment by analysing the FFT of images as they are acquired: residual grating patterns will be evident in the frequency domain as a series of spots corresponding to the zero and first order diffraction points.

SIM is advantageous as it can be carried out with standard fluorophores with no special requirements for sample preparation. The technique is therefore compatible with a variety of powerful existing cytological methods such as fluorescence in situ hybridisation (FISH) and immunolabelling. Furthermore, multicolour imaging is possible simply by repeating acquisition at different excitation wavelengths, although care should be taken to minimise bleaching. Perhaps the most exciting feature of SIM is that the method can be expanded into three dimensions, with optical sectioning achieved by moving the microscope objective in the z-axis. The technique has been used to map interchromatin domains in nuclei in addition to the nuclear lamina of intact nuclei. Whilst the improvement in resolution is only twofold with respect to standard fluorescence microscopy, this improvement is in the axial as well as the lateral dimensions, leading to an 8-fold increase in volumetric resolution. The fact that 3D images can be made with relative ease make SIM a very attractive technique, although care should be taken to minimise artefacts.

2.3 Super-resolution studies of chromatin

The majority of super-resolution chromatin studies have come in the form of 3D-SIM experiments. As little more preparation than normal microscopy is required, carrying out 3D-

SIM seems to be a logical step, compared to the more involved preparation and analysis required for STED and SMLM. Commercial implementations of the latter two technologies mean that they are becoming ever more widespread, and so it will surely not be long until we see more super-resolution studies on chromatin emerging. Naturally there is a teething period as the field accustoms itself to the particularities of each method, however there is much room for exciting innovation with both SMLM and STED.

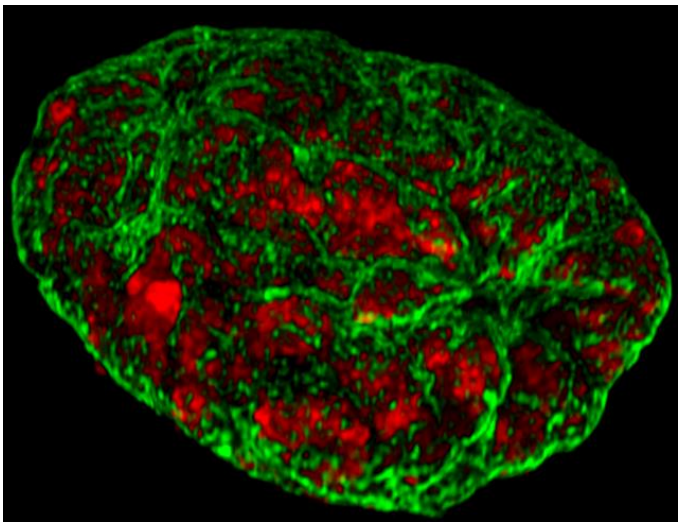

Figure 5

Reproduced form Schermelleh et al.,[55] *a HeLa nucleus in the metaphase. DNA, corresponding to chromatin, is visible in red, the nuclear lamina marked with antibodies is in green. Invaginations of the nuclear envelope are evident in more detail than with a conventional microscope.*

Notable studies using SIM on chromatin include works by Cremer *et al.* on 3D-FISH.[54] Fluorescence in situ hybridisation is a powerful technique, allowing for specific sequences to be labelled with fluorescent dyes. Multicolour FISH (mFISH) is especially useful, allowing for individual chromosomes in a nucleus to each be labelled with a different colour. The technique requires denaturation of DNA to allow the FISH probe to hybridise with the target DNA, and so will necessarily alter the structure of DNA at the molecular level. This is a concern for very high-resolution methods, however it is addressed by Cremer in this publication: minor damage to the nuclear superstructure is noticed after labelling by mFISH and we are advised to be cautious when replicating the technique. SIM images of nuclei labelled with whole chromosome probes show the well-defined interchromosomal boundaries in remarkable detail, opening up the study of nuclei to more ambitious mFISH-SIM experiments – for example, the labelling of individual related genes using FISH would allow their position within the nucleus to be determined with unrivalled precision.

Schermelleh in 2008 used the non-covalent DNA stain DAPI and antibodies targeting nuclear lamin to image HeLa cell nuclei in unprecedented detail in 3D (figure 5).[55] Using segmentation, the group were able to display the organisation of mitotic chromosomes and invaginations by the nuclear envelope into the interchromatin domain. Smeets, with the Cremer laboratory, used

a great number of epigenetic markers to demonstrate the compartmentalised nature of the nucleus.[56] This study exploited the potential for multicolour imaging in SIM, with several markers imaged sequentially to build up In addition to providing further evidence for well-defined 'chromosomal territories', the research showed how the Barr body, the name given to the inactive X chromosome in female cells, interacts with these territories. In each of these cases, the increase in resolution afforded by SIM allowed details not observed in standard fluorescence microscopy to be elucidated.

STED and SMLM have been used to a far lesser extent in the study of chromatin than SIM, however important results have been obtained. Using pulse labelling (see section 4.1), Cseresnyes *et al.* were able to show that origins of DNA replication comprised small clusters of three to five loci, whereas previously origins could only be resolved as larger single points.[57] This observation lends credence to the theory that rather than there being a specific point where replication begins in a given region, any one of a number of proximal locations can 'fire', perhaps simultaneously, to ensure that there is sufficient redundancy for replication to be initiated successfully.

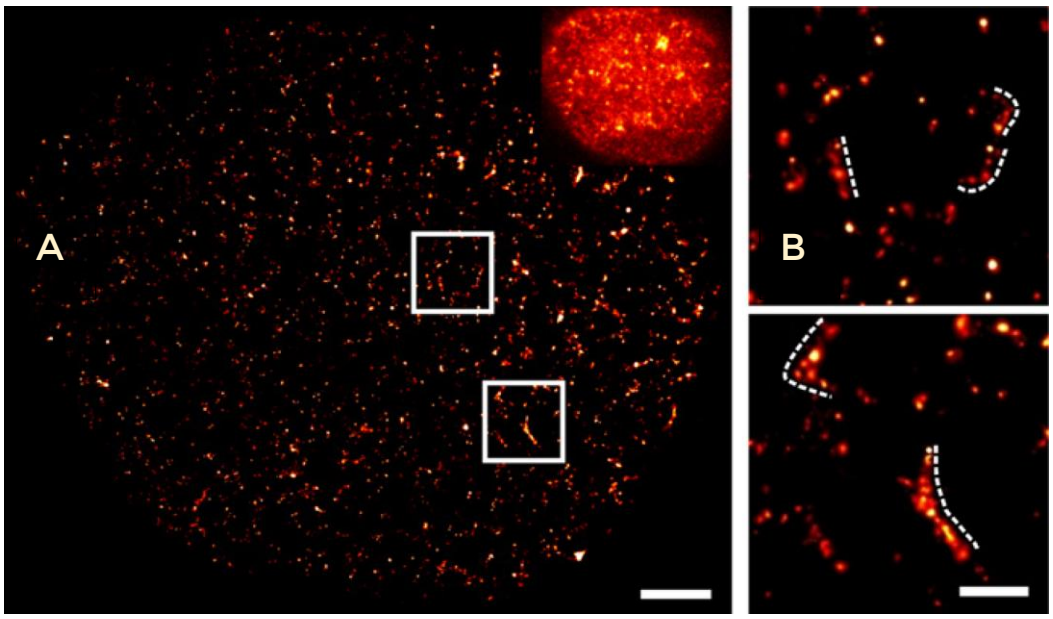

Figure 6

(A) SMLM image of a HeLa nucleus pulse labelled with EdU for 15 minutes and detected with Alexa 647. Widefield image of the same nucleus inset. There is a clear improvement in resolving power with respect to the widefield image; much smaller features can be made out clearly. (B) and (C) Regions within white boxes enlarged. Scale bar 500 nm; dotted white lines show discrete chromatin fibres. Reproduced from Zessin et al.[58]

Again, using pulse labelling, Zessin *et al.* visualised replication regions in HeLa cells pulse labelled for different lengths of time with EdU, this time with SMLM.[58] Subsequent clustering analysis using Ripley's K-function showed that the observed domains became larger with longer

pulse labelling. The group were also able to discern chromatin fibres of roughly 600 nm in length, corresponding to 20 kbp (figure 6.B, 6.C). Beyond these reports, there are few examples of SMLM being used to study human chromatin structure. SMLM therefore presents an exciting opportunity to investigate chromatin, and we hope that by employing replication labelling and eventually synchronisation we will be able to selectively label origins of replication that fire at various points during S-phase.

3. Application of SIM to the study of metaphase chromosomes

4.1 Methods

In order to label DNA with dyes appropriate for super-resolution methods such as STORM and STED, we employ 'replication labelling'. Rather than a fluorescent dye binding in a non-covalent manner to DNA, as with popular DNA stains such as DAPI and the Hoechst family of dyes,[59,60] nucleotide analogues containing a reactive moiety are incorporated into the genome during DNA synthesis, hence the use of the term replication – the incorporation of the target probe occurs during the DNA replication phase of the cell cycle (synthesis-phase, or S-phase).[61] The probe's reactive moiety can be targeted by a modified laser dye with a specific reactive group. A recently-developed implementation of Sharpless's 'click' chemistry[62] is favoured for the labelling step: a terminal alkyne moiety on the sample of interest undergoes a 1,3-cycloaddition with an azide group on a fluorescent dye. A copper (I) catalyst allows the reaction to be performed at room temperature with near-quantitative yield – this is particularly useful within the context of biological specimens, where even only slightly harsh reaction conditions can easily damage tissue and/or biomolecules. Another useful feature of the reaction is its 'bio-orthoganality' – both the alkyne and azide group are seldom found in nature, and so are unlikely to interfere with the biochemistry of the sample.[63] Only the probe incorporated artificially will be targeted for labelling, therefore.

Replication labelling is by no means a new technique. In the 1960s and 1970s, pioneering experiments by Schmid,[64] Taylor,[65] Dutrillaux[66] and Latt[67] allowed the origins of replication to be visualised on chromosomes for the first time. Initially, radioactive ^{3}H-thymidine was used as a marker,[68] however the less hazardous bromodeoxyuridine (BrdU) also began to be used.[66] The use of BrdU is advantageous as its incorporation can be detected with fluorescence, as opposed to ^{3}H-thymidine which limits imaging to film detection or requires the use of a scintillator.[69,70] Staining of chromatin by non-covalent DNA-binding dyes is inhibited in areas where BrdU is incorporated, leading to 'negative' images where a lack of signal implies the presence of BrdU.[66] A more reliable form of detection is immunolabelling, and fluorescent antibodies exist for most thymidine analogues, giving a positive signal where the analogue is incorporated.[71] Further

improvements come with EdU, where, as mentioned above, efficient click chemistry allows for simple labelling of incorporated analogues.

The marking of replicated DNA can be exploited in a number of different ways. Imaging of replication labelling in mitotic chromosomes yields a series of stripes known as 'replication bands'. This allows for the qualitative association between regions of the genome and a given time of replication in the S-phase of the cell cycle generally divided into three parts, early, mid and late. Those bands which appear when a nucleotide analogue is incorporated for the first, middle and latter part of S-phase are called early-replicating, mid-replicating and late-replicating bands respectively. If a cell is stopped before metaphase, it is possible to view marked DNA on the non-condensed chromosomes, and this method has been used to show the distribution of early-, mid- and late-replicating DNA in the nucleus. Generally, a nucleotide analogue must be present for at least a one-hour 'pulse' for homogeneous bands to form on mitotic chromosomes.

Shorter pulses – between one and thirty minutes in length – are often used to observe the sites on the genome where replication begins (replication origins). In a seminal publication, Jackson and Pombo[72] demonstrated that clusters of replication origins, or replicon clusters, are stable throughout several generations, indicating that they may have a function beyond being a trigger for replication in a given region of the genome. Indeed, it has been suggested that replicon clusters are intimately connected with a nuclear matrix which guides chromatin within the nucleus. The implication here is that replicons form part of a monitoring system within the nucleus that ensures the successful replication of DNA within different chromatin domains.

Replication labelling is a very powerful labelling method – its scope ranges from the marking of minuscule numbers of base pairs to the labelling of practically the entire genome, with both consistency and repeatability. Combined with good control over cell synchronisation, it is possible in theory to label any section of the genome required. It should be noted, however, that in asynchronous cell populations, the distribution of cells throughout S-phase means that short pulses can be used to probe every step of S-phase simultaneously. In the context of super-resolution imaging, in particular SMLM, replication labelling fulfils the requirement for discrete structures to be labelled, which is not the case for other methods of DNA labelling. Should SMLM advance to the point where any very densely-labelled sample can be imaged with ease – a distinct possibility considering the advances made in image processing in recent years – then replication labelling should also provide a convenient way of labelling large contiguous sections of chromatin. Here, as a preliminary experiment, we label chromosomes with EdU throughout the whole of S-phase, covering the whole genome, and detect the probe with Alexa Fluor 488 for imaging with SIM.

4.2 Experimental section

4.2.1 Sample preparation

Cells were suspended in RPMI 1640 medium and allowed to reach 50% confluency. To a 150 cm^3 cell culture was added 5-ethynyl-2'-deoxyuridine to a final concentration of 10 µM and colcemid to a final concentration of 0.27 µM. The cell culture was incubated at 37°C in an atmosphere containing 5% CO_2 for 18 hours. After this time, a standard metaphase chromosome spreading procedure was carried out: cells were twice centrifuged (5 minutes, 1200 RPM) and washed with PBS, then suspended in 75 mM KCl aqueous solution for 20 minutes at 37°C. After further centrifugation, the cells were washed twice in a cooled (5°C) 3:1 mixture of methanol and acetic acid (methacarn solution) before being stored at -20°C in methacarn for future use. When required, a 15 µL volume of the cells suspended in methacarn was dropped onto glass coverslips from a height of ~30 cm to allow for chromosome separation. Once the methacarn solution had evaporated, 'click' chemistry labelling of the DNA was performed. A solution for carrying out the 'click' reaction was made: to 2.2 mL of 50 mM tris-buffered saline (pH 7) was added 100 µL of a 100 mM aqueous stock solution of copper sulphate, 250 µL of a 100 mM aqueous stock solution of sodium ascorbate and 1.25 µL of a stock 10 mM solution of Alexa Fluor 488 azide (final concentrations – 4 mM copper sulphate, 10 mM sodium ascorbate, 5 µM Alexa Fluor 488 azide). 0.5 mL of this solution was added to each of the sample-loaded coverslips, which were then left at room temperature in the dark for 30 minutes. Coverslips were then rinsed three times in PBS to remove the reaction solution. 20 µL of the PVA mounting medium was added to glass slides and, when dry, the coverslips mounted on the glass slides. Coverslips were fixed on the glass slides using nail varnish.

4.2.2 Imaging

SIM imaging was carried out on a Zeiss Elyra SIM/STORM microscope. SIM images were acquired with a 100 X magnification objective (NA = 1.4). Samples were mounted on glass coverslips (thickness 1.5) on glass slide substrates. A mounting solution containing polyvinyl alcohol (PVA) (6 g glycerol, 2.4 g PVA, 12 mL 0.2 M tris-buffered saline, 6 mL H_2O, stirred for 4 hours, heated at 50°C for 10 minutes, centrifuge for 15 minutes at 5000 g, supernatant kept for use) was used to ensure the refractive index of the system was maintained. A sCMOS camera was used to acquire images.

The sample was illuminated with a 488 nm laser line with a 42 µm diffraction grating in the optical path. SIM image reconstruction was carried out in the Zen SIM/PALM suite (Carl Zeiss, Berlin). Further image analysis including Fourier transforms was carried out in the Fiji programme.

4.3 Results

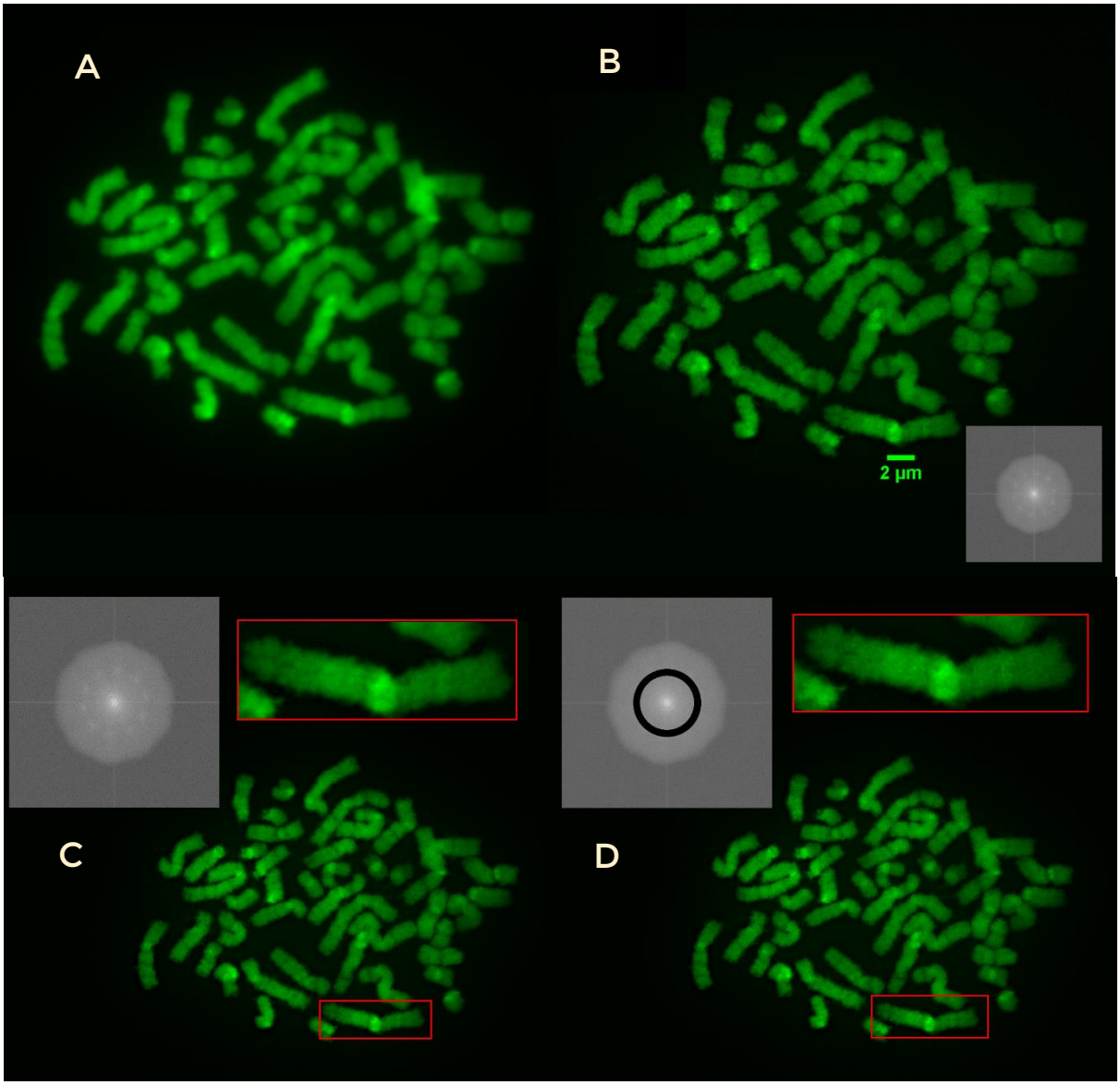

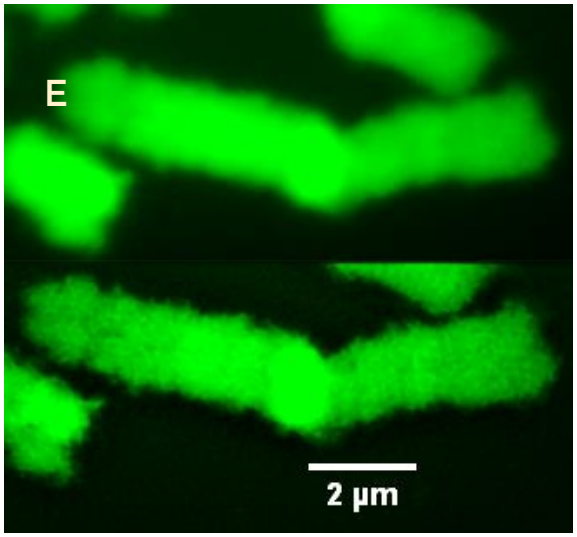

Figure 7

(A) Widefield images of a chromosome spread marked with Alexa Fluor 488. (B) A reconstructed SIM image of the same spread. FFT of the SIM image inset, showing residual structure from the grating. The SIM image seems to show smaller resolvable features than the widefield image. (C) SIM image with FFT and chromosome detail inset. (D) SIM image with grating artefacts removed (FFT inset with grating pattern removed). There is little appreciable difference between the SIM image before and after the removal of grating spots in the FFT, implying that the fine structure seen in the reconstruction is genuine. (E) Comparison of chromosome detail, widefield image top and SIM bottom.

Chromosome spreads were chosen for imaging according to the qualitative extent of labelling observed along the genome. Spreads were also judged according to chromosome number and length. Those selected for SIM imaging displayed 'full' labelling by EdU along their entire length and were not overly compact. Diffraction-limited images (figure 7.A) clearly show metaphase chromosomes, but intensity along the length of the chromosomes is generally uniform. Certain regions appear to have brighter intensity; these are consistent with more densely-packed centromeres and heterochromatin blocks. A SIM reconstruction shows more well-defined features within each chromosome (figure 7.B). It is important to note that the images taken are projections through the whole structure of the chromosome; although it may appear that the structures form the surface of the chromosome, it is possible that this is not the case. The features observed are on the order of 150 nm x 150 nm, which is consistent with the improvement in resolution one would expect to see with SIM. It is also possible to see features protruding from the chromosomes (figure 7.E). These strands have a width of approximately 150 nm, consistent with chromatin 'loops' seen to protrude from metaphase chromosomes seen in electron microscopy. In general, the features observed in the reconstructed SIM image are broadly consistent with SEM images of metaphase chromosomes (see figure 8 for comparison).[73]

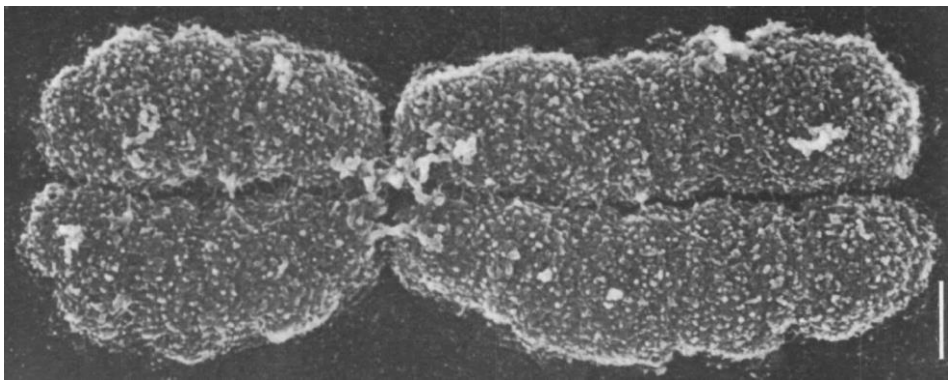

Figure 8

SEM image of human chromosome reproduced from Harrison et al.,[73] *scale bar 500 nm. There is a resemblance between the SEM and our SIM images, however care must be taken when interpreting these data – SEM provides a surface image, whilst SIM shows a projection through the whole sample. It is possible that the loops projecting from the chromatin are equivalent in SEM and SIM images.*

For quality control, Fourier transforms were made of the reconstructed images. For the first spread, the spatial frequency image contained a regular pattern which is an artefact of the structured illumination (figure 7.B, 7.C). Such artefacts are common: residual grating patterns can easily occur if illumination is not uniform as the grating is rotated, or equally if bleaching of the dyes causes variations in intensity. In order to ascertain whether this meant the 150 nm structures in the real space image resulted from the structured illumination, a torus containing the grating pattern was cropped from the Fourier space image and an inverse FFT performed

(figure 7.D). The resulting real space image still displayed the 150 nm chromatin structures, and so we could be confident that the newly-resolved features were real.

When imaging the second spread (figure 9), we ensured that illumination reached a constant level by irradiating the sample with laser light for two minutes. We hoped that this would reduce the likelihood of grating artefacts by bleaching fluorophores susceptible to degradation before rather than during the acquisition. The FFT of the real space reconstruction showed no such grating artefact (figure 9.B), and so again it can be assumed that the structures seen in the image are not the result of the imaging method.

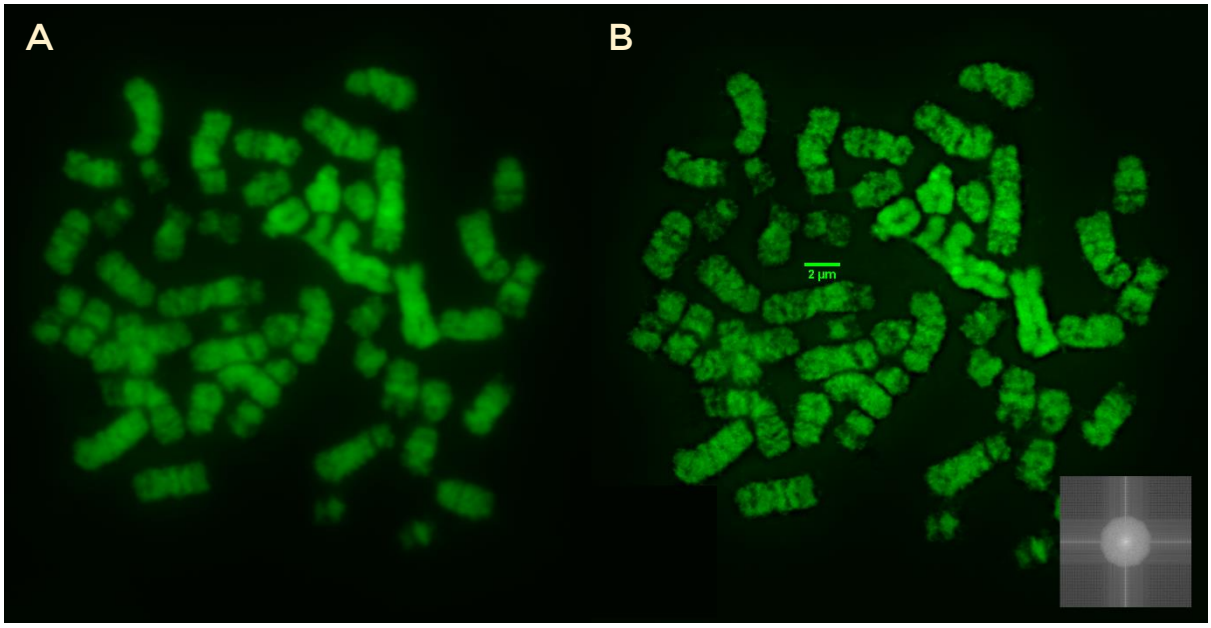

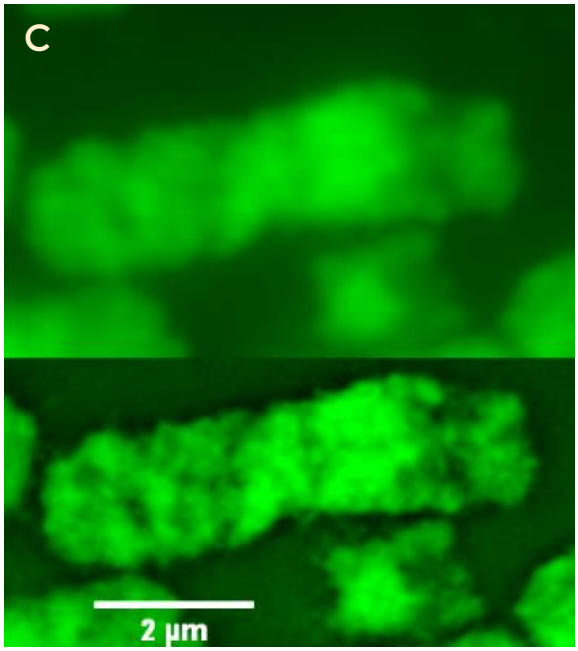

Figure 9

Second chromosome spread prepared in the same manner as the first. (A) Widefield image. (B) SIM reconstruction of the same spread, FFT of image inset. (C) Detail of chromosome, widefield top and SIM reconstruction bottom. There is a clear increase in resolution, with small features on the order of 150 nm present in the chromatin. Features of a similar size between the chromosomes could be from residual cytoplasm.

More worrying, perhaps, is the presence of structures similar to those observed within the chromosomes on the background of the image, especially in the spaces between chromosomes. It is possible that the observed structures are an artefact of the sample preparation. It has been observed in SEM imaging of mammalian metaphase cells that residual cytoplasm covers chromosome spreads.[74] Heretofore this has not been considered a problem in optical microscopy as the cytoplasmic layer is not seen under epifluorescence. We speculate, however, that EdU could remain in the nucleus after the cell fixation, and these remnants could be marked with fluorescent dye during the labelling procedure. A low concentration of Alexa Fluor 488-marked EdU may only show up as a uniform background signal under a standard microscope, however in SIM it is possible that a distribution of dye molecules in the cytoplasm is visible. In order to verify whether or not this is the case, there are several options we can take. The simplest is to modify the sample preparation to include a specific washing step to remove cell cytoplasm. This is possible using commercially available products (often a mixture of detergents which remove lipids and glycoproteins found in cytoplasm), although this step could certainly lead to the formation of more artefacts through the traumatic nature of the washing step. Alternatively, a different staining method, using a non-covalent DNA stain, could be employed. DNA minor groove binders such as DAPI may not bind to species in the cytoplasm to the same extent as the Alexa Fluor 488 to EdU, however a price to pay would be the lower fluorescence efficiency of DAPI.

We did not carry out z-stack imaging of either of the two spreads imaged. The samples were not prepared in a way that preserves three-dimensional structure of the chromosomes – air drying leads to collapse of the chromatin and so little useful information would be obtained. In future, however, we hope to employ 3D-SIM as a matter of course. This in turn would help us to ascertain whether or not cytoplasmic residues cover chromosomes and lead to the features observed.

4. Conclusions and outlook

SIM shows encouraging signs for the study of chromosomes and chromatin beyond the diffraction limit. There is a clear improvement in resolution over the widefield fluorescence image, as should be expected. However, resolution is still limited to 150 nm, which is not enough to study the higher-order chromatin structures of real interest. Furthermore, as increasing resolution shows, we must be wary of sample preparation artefacts – these will only become more obvious at higher resolutions.

Biology has been dominated in recent years by the human genome project, perhaps at the expense of structural studies. Structural biology has also been limited by the 'optical gap', the region between X-ray crystallography and the diffraction limit where effectively no images can be made. Now that super-resolution is becoming widespread, it is very likely that the optical gap will become a thing of the past. Whilst electron microscopy is powerful and can resolve features on the nanometre scale, the harsh sample preparation associated with EM limit its scope. Furthermore, it is clear that variety of labels available for optical microscopy makes it superior to EM, which often lacks gene- or protein-specific labels.

It is certain that, provided sample preparation is optimised to take into account the quirks of SIM, STED and SMLM, the combined availability of super-resolution methods for the study makes them a very powerful tool for the study of chromatin.

5. References

1. Wanner, G., Schroeder-Reiter, E. & Formanek, H. 3D analysis of chromosome architecture: advantages and limitations with SEM. *Cytogenet. Genome Res.* **109,** 70–8 (2005).
2. Wanner, G. & Schroeder-Reiter, E. Scanning electron microscopy of chromosomes. *Methods Cell Biol.* **88,** 451–74 (2008).
3. Dwiranti, A. *et al.* The Effect of Magnesium Ions on Chromosome Structure as Observed by Helium Ion Microscopy. *Microsc. Microanal.* **20,** 184–188 (2013).
4. Ushiki, T. & Hoshi, O. Atomic force microscopy for imaging human metaphase chromosomes. *Chromosome Res.* **16,** 383–96 (2008).
5. Nishino, Y., Takahashi, Y., Imamoto, N., Ishikawa, T. & Maeshima, K. Three-Dimensional Visualization of a Human Chromosome Using Coherent X-Ray Diffraction. *Phys. Rev. Lett.* **102,** 018101 (2009).
6. Giewekemeyer, K. *et al.* Quantitative biological imaging by ptychographic x-ray diffraction microscopy. *Proc. Natl. Acad. Sci. U. S. A.* **107,** 529–34 (2010).
7. Strick, R., Strissel, P. L., Gavrilov, K. & Levi-Setti, R. Cation-chromatin binding as shown by ion microscopy is essential for the structural integrity of chromosomes. *J. Cell Biol.* **155,** 899–910 (2001).
8. Joti, Y. *et al.* Chromosomes without a 30-nm chromatin fiber. *Nucleus* **3,** 404–410 (2012).
9. Ilatovskiy, A. V, Lebedev, D. V, Filatov, M. V, Petukhov, M. G. & Isaev-Ivanov, V. V. SANS spectra of the fractal supernucleosomal chromatin structure models. *J. Phys. Conf. Ser.* **351,** 012007 (2012).
10. Dekker, J., Rippe, K., Dekker, M. & Kleckner, N. Capturing chromosome conformation. *Science* **295,** 1306–11 (2002).
11. Hakim, O. & Misteli, T. SnapShot: Chromosome confirmation capture. *Cell* **148,** 1068.e1–2 (2012).
12. Dostie, J. & Dekker, J. Mapping networks of physical interactions between genomic elements using 5C technology. *Nat. Protoc.* **2,** 988–1002 (2007).
13. Belton, J.-M. *et al.* Hi-C: a comprehensive technique to capture the conformation of genomes. *Methods* **58,** 268–76 (2012).
14. Imakaev, M. *et al.* Iterative correction of Hi-C data reveals hallmarks of chromosome organization. *Nat. Methods* **9,** 333–1003 (2012).
15. De Wit, E. & de Laat, W. A decade of 3C technologies: insights into nuclear organization. *Genes Dev.* **26,** 11–24 (2012).
16. Naumova, N. *et al.* Organization of the Mitotic Chromosome. *Science (80-.).* **948,** (2013).
17. Nagano, T. *et al.* Single-cell Hi-C reveals cell-to-cell variability in chromosome structure. *Nature* **502,** 59–64 (2013).
18. Abbe, E. Beiträge zur Theorie des Mikroskops und der mikroskopischen Wahrnehmung. *Arch. für mikroskopische Anat.* **9,** 413–418 (1873).
19. Garini, Y., Vermolen, B. J. & Young, I. T. From micro to nano: recent advances in high-

resolution microscopy. *Curr. Opin. Biotechnol.* **16,** 3–12 (2005).

20. Egner, A. & Hell, S. W. Fluorescence microscopy with super-resolved optical sections. *Trends Cell Biol.* **15,** 207–15 (2005).

21. Rittweger, E., Han, K. Y., Irvine, S. E., Eggeling, C. & Hell, S. W. STED microscopy reveals crystal colour centres with nanometric resolution. *Nat. Photonics* **3,** 144–147 (2009).

22. Hein, B., Willig, K. I. & Hell, S. W. Stimulated emission depletion (STED) nanoscopy of a fluorescent protein-labeled organelle inside a living cell. *Proc. Natl. Acad. Sci.* **105 ,** 14271–14276 (2008).

23. Lalkens, B., Testa, I., Willig, K. I. & Hell, S. W. MRT letter: Nanoscopy of protein colocalization in living cells by STED and GSDIM. *Microsc. Res. Tech.* **75,** 1–6 (2012).

24. Hell, S. W. Toward fluorescence nanoscopy. *Nat. Biotechnol.* **21,** 1347–55 (2003).

25. Abbott, A. The Glorious Resolution. *Nature* **459,** 4–5 (2009).

26. Chmyrov, A. *et al.* Nanoscopy with more than 100,000 "doughnuts". *Nat. Methods* **10,** 737–40 (2013).

27. Bingen, P., Reuss, M., Engelhardt, J. & Hell, S. W. Parallelized STED fluorescence nanoscopy. *Opt. Express* **19,** 23716–26 (2011).

28. Rowlands, C. J., Yew, E. Y. S. & So, P. T. C. Parallel super-resolution imaging. *Nat. Methods* **10,** 709–10 (2013).

29. Rust, M. J., Bates, M. & Zhuang, X. Sub-diffraction-limit imaging by stochastic optical reconstruction microscopy (STORM). *Nat. Methods* **3,** 793–795 (2006).

30. Testa, I. *et al.* Multicolor fluorescence nanoscopy in fixed and living cells by exciting conventional fluorophores with a single wavelength. *Biophys. J.* **99,** 2686–94 (2010).

31. Dempsey, G., Vaughan, J., Chen, K., Bates, M. & Zhuang, X. Evaluation of fluorophores for optimal performance in localization-based super-resolution imaging. *Nat. Methods* **8,** (2011).

32. Deschout, H. *et al.* Precisely and accurately localizing single emitters in fluorescence microscopy. *Nat. Methods* **11,** 253–66 (2014).

33. Dedecker, P., Duwé, S., Neely, R. K. & Zhang, J. Localizer: fast, accurate, open-source, and modular software package for superresolution microscopy. *J. Biomed. Opt.* **17,** (2012).

34. Smith, C. S., Joseph, N., Rieger, B. & Lidke, K. a. Fast, single-molecule localization that achieves theoretically minimum uncertainty. *Nat. Methods* **7,** 373–5 (2010).

35. Nieuwenhuizen, R. P. J. *et al.* Measuring image resolution in optical nanoscopy. *Nat. Methods* **10,** 557–62 (2013).

36. Henriques, R. *et al.* QuickPALM: 3D real-time photoactivation nanoscopy image processing in ImageJ. *Nat. Methods* **7,** 339–40 (2010).

37. Vogelsang, J. *et al.* Make them blink: probes for super-resolution microscopy. *Chemphyschem* **11,** 2475–90 (2010).

38. Baddeley, D., Cannell, M. B. & Soeller, C. Visualization of Localization Microscopy Data. *Microsc. Microanal.* 64–72 (2010).

39. Herbert, S., Soares, H., Zimmer, C. & Henriques, R. Single-molecule localization super-resolution microscopy: deeper and faster. *Microsc. Microanal.* **18,** 1419–1429 (2012).

40. Van de Linde, S. & Sauer, M. How to switch a fluorophore: from undesired blinking to controlled photoswitching. *Chem. Soc. Rev.* **43,** 1076–87 (2014).

41. Mukamel, E. a, Babcock, H. & Zhuang, X. Statistical deconvolution for superresolution fluorescence microscopy. *Biophys. J.* **102,** 2391–400 (2012).

42. Cox, S. *et al.* Bayesian localization microscopy reveals nanoscale podosome dynamics. *Nat. Methods* **9,** (2012).

43. Rosten, E., Jones, G. E. & Cox, S. ImageJ plug-in for Bayesian analysis of blinking and bleaching. *Nat. Methods* **10,** 97–8 (2013).

44. Holden, S. J., Uphoff, S. & Kapanidis, A. N. DAOSTORM: an algorithm for high- density super-resolution microscopy. *Nat. Methods* **8,** 279–80 (2011).

45. Min, J. *et al.* FALCON: fast and unbiased reconstruction of high-density super-resolution microscopy data. *Sci. Rep.* **4,** 4577 (2014).

46. Vogelsang, J., Cordes, T., Forthmann, C., Steinhauer, C. & Tinnefeld, P. Controlling the fluorescence of ordinary oxazine dyes for single-molecule switching and superresolution microscopy. *Proc. Natl. Acad. Sci. U. S. A.* **106,** 8107–12 (2009).

47. Bates, M., Huang, B., Dempsey, G. T. & Zhuang, X. Multicolor super-resolution imaging with photo-switchable fluorescent probes. *Science* **317,** 1749–53 (2007).

48. Blom, H. & Widengren, J. Blurry vision belongs to history. *Physics (College. Park. Md).* **3,** 40 (2010).

49. Heintzmann, R. in *Handb. Biol. Confocal Microsc.* (Pawley, J. B.) (Springer Science+Business Media, 2006).

50. Gustafsson, M. G. Surpassing the lateral resolution limit by a factor of two using structured illumination microscopy. *J. Microsc.* **198,** 82–7 (2000).

51. Carlton, P. M. Three-dimensional structured illumination microscopy and its application to chromosome structure. *Chromosome Res.* **16,** 351–65 (2008).

52. Jost, A. & Heintzmann, R. Superresolution Multidimensional Imaging with Structured Illumination Microscopy. *Annu. Rev. Mater. Res.* **43,** 261–282 (2013).

53. Schaefer, L. H., Schuster, D. & Schaffer, J. Structured illumination microscopy: Artefact analysis and reduction utilizing a parameter optimization approach. *J. Microsc.* **216,** 165–174 (2004).

54. Markaki, Y. *et al.* The potential of 3D-FISH and super-resolution structured illumination microscopy for studies of 3D nuclear architecture: 3D structured illumination microscopy of defined chromosomal structures visualized by 3D (immuno)-FISH opens new perspectives for stud. *Bioessays* **34,** 412–26 (2012).

55. Schermelleh, L. *et al.* Subdiffraction multicolor imaging of the nuclear periphery with 3D structured illumination microscopy. *Science* **320,** 1332–6 (2008).

56. Smeets, D. *et al.* Three-dimensional super-resolution microscopy of the inactive X chromosome territory reveals a collapse of its active nuclear compartment harboring distinct Xist RNA foci. *Epigenetics Chromatin* **7,** 8 (2014).

57. Cseresnyes, Z., Schwarz, U. & Green, C. M. Analysis of replication factories in human cells by super-resolution light microscopy. *BMC Cell Biol.* **10,** 88 (2009).

58. Zessin, P. J. M., Finan, K. & Heilemann, M. Super-resolution fluorescence imaging of chromosomal DNA. *J. Struct. Biol.* **177,** 344–8 (2012).

59. Kapuscinski, J. DAPI: a DNA-specific fluorescent probe. *Biotech. Histochem.* **70,** 220–33 (1995).

60. Fornander, L. H., Wu, L., Billeter, M., Lincoln, P. & Nordén, B. Minor-groove binding drugs: where is the second Hoechst 33258 molecule? *J. Phys. Chem. B* **117,** 5820–30 (2013).

61. Chehrehasa, F., Meedeniya, A. C. B., Dwyer, P., Abrahamsen, G. & Mackay-Sim, A. EdU, a new thymidine analogue for labelling proliferating cells in the nervous system. *J. Neurosci. Methods* **177,** 122–30 (2009).

62. Kolb, H. C., Finn, M. G. & Sharpless, K. B. Click Chemistry: Diverse Chemical Function from a Few Good Reactions. *Angew. Chemie Int. Ed.* **40,** 2004–2021 (2001).

63. Sletten, E. M. & Bertozzi, C. R. Bioorthogonal Reactions. *Acc. Chem. Res.* **44,** 666–676 (2011).

64. Schmid, W. DNA replication patterns of human chromosomes. *Cytogenetics* **2,** 175–193 (1963).

65. Taylor, J. H. Asynchronous duplication of chromosomes in cultured cells of Chinese hamster. *J. Biophys. Biochem. Cytol.* **7,** 455–64 (1960).

66. Dutrillaux, B., Couturier, J., Richer, C. L. & Viegas-Péquignot, E. Sequence of DNA replication in 277 R- and Q-bands of human chromosomes using a BrdU treatment. *Chromosoma* **58,** 51–61 (1976).

67. Latt, S. a, Willard, H. F. & Gerald, P. S. BrdU-33258 Hoechst analysis of DNA replication in human lymphocytes with supernumerary or structurally abnormal X chromosomes. *Chromosoma* **57,** 135–53 (1976).

68. Woods, P. S., Gay, H. & A, S. Organization of the Salivary-Gland Chromosome as Revealed by the Pattern of Incorporation of H3-Thymidine. *Proc. Natl. Acad. Sci. U. S. A.* **47,** 1486–1493 (1961).

69. Caspary, E. A. & Hughes, D. Liquid scintillation counting techniques in lymphocyte transformation in vitro measured by tritiated thymidine uptake. *J. Immunol. Methods* **1,** 263–272 (1972).

70. Cavanagh, B. L., Walker, T., Norazit, A. & Meedeniya, A. C. B. Thymidine analogues for tracking DNA synthesis. *Molecules* **16,** 7980–7993 (2011).

71. Vogel, W., Autenrieth, M. & Mehnert, K. Analysis of chromosome replication by a BrdU antibody technique. *Chromosoma* **98,** 335–41 (1989).

72. Jackson, D. A. & Pombo, A. Replicon Clusters Are Stable Units of Chromosome Structure: Evidence That Nuclear Organization Contributes to the Efficient Activation and Propagation of S Phase in Human Cells. *J. Cell Biol.* 1285–1295 (1998).

73. Harrison, C. J., Allen, T. D., Britch, M. & Harris, R. High-resolution scanning electron microscopy of human metaphase chromosomes. *J. Cell Sci.* **56,** 409–22 (1982).

74. Shemilt, L. A., Estandarte, A. K. C., Yusuf, M. & Robinson, I. K. Scanning electron microscope studies of human metaphase chromosomes. *Philos. Trans. A. Math. Phys. Eng. Sci.* **372,** (2014).